Observation and assignment of a high-resolution FTIR-spectrum of T$_2^{16}$O, DT^{16}O and HT^{16}O in the range of 4300 to 4700 cm^{-1}

Valentin Hermann [a],*, Anne Freise [a], Magnus Schlösser [a], Frank Hase [b], Johannes Orphal [b]

[a] Tritium Laboratory Karlsruhe (TLK), Institute for Astroparticle Physics (IAP), Karlsruhe Institute of Technology (KIT), Karlsruhe, Germany
[b] Institute of Meteorology and Climate Research (IMK) - Atmospheric Trace Gases and Remote Sensing (ASF), Karlsruhe Institute of Technology (KIT), Karlsruhe, Germany

ARTICLE INFO

ABSTRACT

In the range of 4300 to 4700 cm^{-1}, we present analysis of the $2\nu_1$, $2\nu_2+\nu_3$ and $\nu_1+\nu_3$ bands of T$_2^{16}$O, the $2\nu_1$ and $\nu_1+2\nu_2$ of DT^{16}O and the $2\nu_1$ of HT^{16}O. The analysed high-resolution spectrum has been obtained from a Bruker IFS 125HR Fourier-transform spectrometer with a resolution of 0.025 cm^{-1} using an optical cell with an activity of 10 GBq. For the in total 2436 lines an individual positional uncertainty of up to 3.4×10^{-5} cm^{-1} and a systematic uncertainty of 7.5×10^{-4} cm^{-1} could be achieved. Four of the six bands have been analysed for the first time, the $\nu_1+\nu_3$ band of T$_2^{16}$O and the $2\nu_1$ of HT^{16}O have been analysed in previous works of our group. These datasets are extended by 527 new lines and a cross check is confirming the consistency between both works. A comparison of the assigned line positions to the variationally calculated predictions from the Tomsk database agrees with previous findings indicating that band-specific shifts and shifts depending on the rotational quantum numbers are observed leading to an overall difference of up to 0.3 cm^{-1}.

1. Introduction

The radioactive hydrogen isotope tritium is of interest in multiple research disciplines. It is used to directly determine the neutrino mass from high-precision electron spectroscopy of its beta decay [1,2], it is the fuel in future fusion reactors [3] and in molecular spectroscopy it can be used for fundamental tests of quantum mechanics as the strong isotopic effect of $^1H = H$, $^2H = D$ and $^3H = T$ allow for testing mass-dependent adiabatic and non-adiabatic contributions [4–6]. For some of these aspects tritiated water is playing a special role demanding a highly accurate and complete data base for the tritiated water isotopologues as well. On the one hand, the water molecule itself is studied in fundamental theoretical investigations [7], and on the other hand, the highly radiotoxic vapour of its tritiated species is generated during processes with tritium and has to be monitored precisely [8–10] for safety reasons. Some experimental studies on the tritiated water isotopologues have been performed [11–20] prior to efforts by our group.

In this work, we present measurements from a high-resolution FTIR-spectrum: the $2\nu_1$, $2\nu_2+\nu_3$ and $\nu_1+\nu_3$ bands from the T$_2^{16}$O species, the $2\nu_1$ and the $\nu_1+2\nu_2$ from the DT^{16}O species and the $2\nu_1$ of the HT^{16}O species. Four of the six bands have been analysed for the first time, while the $\nu_1+\nu_3$ band of T$_2^{16}$O and the $2\nu_1$ of HT^{16}O have been analysed

previously [21,22], but are extended by using an improved sample for the measurement.

For all bands, we present line lists, a comparison to variational calculations, the spectroscopic constants for the A-reduced Watson Hamiltonian of the ground state and for the $\nu_1+\nu_3$ band of T$_2^{16}$O and the $2\nu_1$ of HT^{16}O a comparison to previous assignments.

2. Experiment

2.1. Experimental setup and acquisition of spectrum

The analysed spectrum has been recorded by a Fourier-transform spectrometer Bruker IFS 125HR at a resolution of 0.025 cm^{-1}. A near-nominal instrumental line shape has been ensured by performing regular checks of the alignment status of the FTIR spectrometer using gas samples filled with HCl, C$_2$H$_2$, or N$_2$O [23,24]. These resulting spectra were analysed using the LINEFIT software [25].

For the measurement of the tritiated water isotopologues a special spectroscopic cell has been developed complying with the tritium specific requirements for material selection and safety. Previously, our employed cell housed a 200 mm long and 4 mm diameter high-reflective aluminium light-pipe [26]. It has been shown that this geometry leads

---
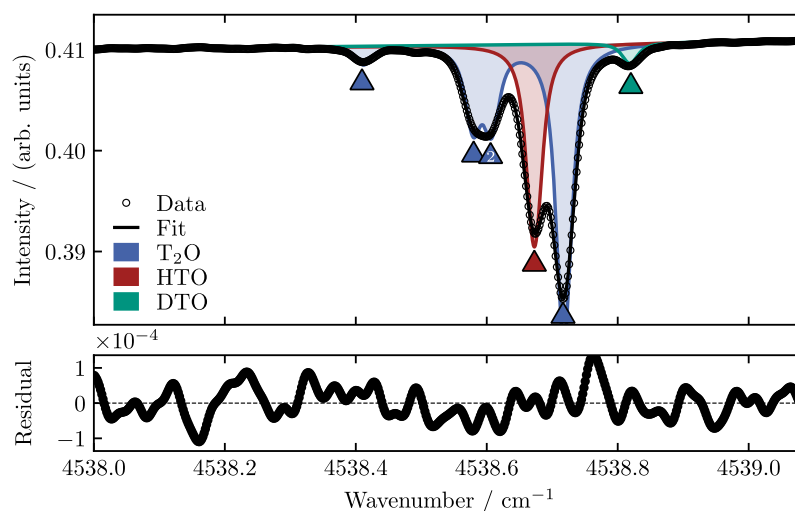
Fig. 1. Example of a slice of the measured spectrum with the synthetic spectrum (fit) using the ab-initio predictions of Tomsk [29] for the tritiated water species HTO, DTO and T_2O after the fitting procedure with the minuit algorithm. The positions of the lines are highlighted with markers. The "2" indicates that two lines of this species are in close proximity of the marker's position.

a decent signal-to-noise ratio due to a long beam-path and reasonable sample pressure. For this work, the light-pipe material was exchanged by polished silver which offers enhanced IR reflectivity [21]. The tight geometry restricts the gas sample to a total activity of 10 GBq equivalent to a pressure of about 35 mbar. For the sample preparation, an in-situ synthesis reactor is connected to the light-pipe cell filled with CuO powder and to reduce the protium solved in the components flushed with deuterium. After filling the cell with a deuterium-tritium mixture ($D_2:T_2 = 1 : 3$) with a total activity of 10 GBq the synthesis is performed by heating the reactor to 225 °C and cryo-pumping the water vapour into the light-pipe segment. It has been observed in the previous sample [21,22,26–28] and by Kobayashi [20] that the amount of protium solved in steel components is significant for such experiments why no additional protium has been loaded in the cell. Note that this sample has 10 times the activity of the previous sample. As this value is 10 times the exempted limit for this radioactive isotope, a special license was necessary for performing the experiments.

After synthesis, the spectroscopic cell contains the water isotopologues $HT^{16}O$, $DT^{16}O$, $T_2^{16}O$, $H_2^{16}O$, $HD^{16}O$ and $D_2^{16}O$, as-well as $C^{16}O_2$ usually used for calibration purposes and traces of methane resulting from reactions of the contained gases with the carbon in the steel. By taking the relative line strengths of the water lines and the natural abundance into account, the composition of the hydrogen isotopes is estimated to be almost equal (H:D:T = 33 % : 36 % : 31 %). For the acquisition, an integration of 588 scans of each 30 s has been performed. The range of 4780 to 5175 cm^{-1} of this spectrum has been analysed earlier [21]. The evaluated spectrum ranges from 4300 to 4700 cm^{-1} containing the $2\nu_1$ and $2\nu_2+\nu_3$ bands of $T_2^{16}O$ and the $2\nu_1$ and $\nu_1+2\nu_2$ bands of $DT^{16}O$, all four analysed for the first time and the $\nu_1+\nu_3$ of $T_2^{16}O$ and $2\nu_1$ of $HT^{16}O$.

### 2.2. Wavenumber axis calibration

The calibration of the wavenumber axis is a mandatory procedure taking into account contributions like the finite field-of-view accepted by the interferometer, a minimal misalignment in the FTIR beam path and dispersion effects between the HeNe reference laser wavelength and the infrared region. The interferometer is operated in vented state, as it is mostly used for atmospheric observations In the region between 4200 and 4340 cm^{-1}, the calibration has been performed by comparing the positions of 25 $HD^{16}O$ lines with those from the HITRAN database [30]. For the presented line positions, additional uncertainty resulting from the calibration process has to be included.

The uncertainties on the line positions of the reference lines range according to HITRAN database from $10^{-4} – 10^{-5}$ cm^{-1} and are therefore taken into account as a systematic uncertainty of 1×10^{-4} cm^{-1}. The statistical error on the calibration parameter leads to an uncertainty of 6.5×10^{-4} cm^{-1}. Contributions to the uncertainty due to the fitting process, the pressure shift and the air-broadening have been considered but can be neglected. All sources of uncertainty taken into account a systematic uncertainty of 7.5×10^{-4} cm^{-1} from the calibration has to be added to the individual uncertainties of each line position.

2.3. Line assignments

The line assignment has been performed on slices of the measured spectrum containing up to 10 lines of the target gases $HT^{16}O$, $DT^{16}O$ and $T_2^{16}O$, lines of the other molecules in the sample and lines from absorption in the beam path outside the sample. An example of a slice of the measured spectrum is given in Fig. 1. For each slice a synthetic spectrum is generated by simulating the line profiles using the line parameters of the HITRAN database for the non-tritiated gases and the line positions and (relative) intensities from the theoretical predictions in the Tomsk database [29] for the radioactive water isotopologues. The synthetic spectrum takes into account the convolution of the Voigt profiles of the interfering lines and the response function of the FTIR spectrometer. This model of the spectrum is fitted to the measured spectrum using the robust minimization algorithm MINUIT [31] via the iminuit[1] Python library determining the here presented line intensities and line centres with their individual uncertainties. As observed in earlier works of our group [21,22,27,28] the theoretical predictions of the Tomsk database obtained from variational calculations with the potential energy surface of Partridge and Schwenke [32] deviate from the measured positions with up to ± 0.3 cm^{-1} corresponding to over 20 times the line widths. Despite the comparably large deviations of these calculations, the accuracy of the relative line intensities and the relative distance of lines within a band permit in most cases to perform an initial visual assignment. Due to a high line density in the evaluated spectra, especially for the tritiated water isotopologues, some of the predicted line positions could not be identified unambiguously and have been discarded. The relatively large differences to the theoretical predictions and therefore the need of a visual assignment demands a consistency check of the acquired data set. Therefore, the acquired

---

[1] https://github.com/scikit-hep/iminuit
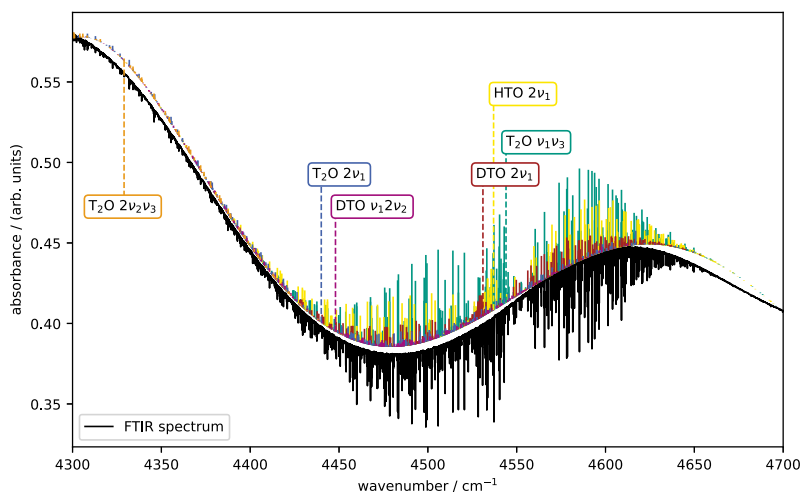
Fig. 2. The assigned lines for each of the four new presented bands and the reassigned $2\nu_1$ of HTO and $\nu_1+\nu_3$ of T$_2$O (all pos. y-scale) are compared in line intensity and position to the measured IR spectrum (neg. y-scale). The band centres are indicated with dashed lines.

Table 1

Overview of the assigned lines of the different tritiated water species to vibrational bands with quantum numbers ν_1, ν_2 and ν_3 for the symmetric stretch, symmetric bend and asymmetric stretch. Some lines of the $2\nu_1$ band of HTO and the $\nu_1+\nu_3$ band of T$_2$O have been analysed in previous studies of our group [21,22]. The mean difference of the line positions to the ab initio predictions from Tomsk database [29] ($\overline{\Delta}_{\text{Tomsk}}$) and the standard deviation are given. A discussion of these differences is provided in the text.

Species	$\nu_1\ \nu_2\ \nu_3$	New lines	Updated lines	$\overline{\Delta}_{\text{Tomsk}}$ (cm^{-1})	STD (cm^{-1})
HT^{16}O	2 0 0	107	347	-0.080	0.048
DT^{16}O	2 0 0	440	–	-0.124	0.029
DT^{16}O	1 2 0	265	–	-0.026	0.033
T$_2^{16}$O	2 0 0	479	–	-0.164	0.040
T$_2^{16}$O	1 0 1	420	206	-0.139	0.039
T$_2^{16}$O	0 2 1	172	–	0.141	0.023

bands are checked for plausibility by reviewing the differences to the predictions of Tomsk in dependency of the quantum numbers and transition energy. A parabolic, quantum number K_a-dependent distribution comparable to previous observations [21,28] is expected which is further discussed it the results section. Then, as second plausibility check for each band the fit of the spectroscopic parameters of the Watson Hamiltonian for the ground state has been performed yielding RMS values for the line positions up to 8.76×10^{-3} cm^{-1}.

3. Results and discussion

3.1. Experimental line list and spectra

In the range from 4300 to 4700 cm^{-1}, 2436 lines have been assigned to ro-vibrational bands of HT^{16}O, DT^{16}O and T$_2^{16}$O. In Table 1 an overview about the assigned bands is given listing new lines and updated lines. As this spectral range has already been analysed before using an optical cell with less tritium and overall lower signal-to-noise [21,22] the earlier HTO ν_2 and T$_2$O $\nu_1+\nu_3$ bands have now been enlarged by 567 lines. A comparison of the 553 common lines is given below.

In this study lines with rotational quantum numbers up to $J' = 19$ and $K_a' = 10$ have been analysed. The individual statistical uncertainties on the line positions of the presented lines resulting from the fitting procedure ranges from 3.4×10^{-5} to 6.8×10^{-2} cm^{-1}. Fig. 2 presents a comparison of the assigned spectral lines of the 6 bands with the measured IR spectrum showing the tritiated water isotopologues to be the dominant source of signal in this range. The band centres are indicated with dashed lines.

For all assigned bands, line lists are given as supplemental material including the line positions, line intensities, their individual uncertainties and the corresponding transition quantum numbers.

3.2. Comparison of the assigned lines with variational calculations

While the prediction of the relative line intensities agree very well with the assignment the line positions deviate up to ± 0.3 cm^{-1}. In Fig. 3, the differences of the observed line positions to those of the ab-initio predictions from the Tomsk database (Tomsk - observed) are plotted over the observed line positions for the example of the $\nu_1 + 2\nu_2$ of DTO and the $2\nu_1$ band of HTO including the uncertainties of the line position. As seen in previous observations [21,22,28] and observed here for each of the six bands, these deviations relate to a band-specific shift that can be negative or positive as displayed in Table 1.

Furthermore, a dependence on the rotational quantum numbers is found. The effect is most visible in J' (and J'') and in K_a' (and K_a'') as visualized in Fig. 4 for the example of the $2\nu_1$ bands of T$_2$O and HTO using $J(J + 1)$ as y-axis and various colours for selected values of K_a'. This dependence has been observed for all bands varying in magnitude for J and K_a. Plots showing the K_a and $J(J + 1)$ dependence for all presented bands can be found in the supplemental material.

3.3. Fit of the spectroscopic parameters to the Watson Hamiltonian

As a consistency check and for the acquisition of the spectroscopic parameters of the ground state, combination differences with the lines of the individual vibrational modes have been found and used, combined with the pure rotational lines of Helminger et al. [12] respectively de Lucia et al. [11], to perform a fit of the non-perturbed Watson Hamiltonian.

The obtained parameters are in good agreement with those acquired by Helminger and de Lucia. The RMS deviations of the line positions of the combination differences resulting from this fit are with $\approx 6 \times 10^{-3}$ cm^{-1} in the order of the stated uncertainties.

Furthermore, we performed fits of Watson Hamiltonian parameters to the upper state of each vibrational mode in HTO, DTO and T$_2$O. These fits only converged with satisfactory outcome for the $2\nu_1$ band of HTO (i.e. RMS deviation of $\approx 3 \times 10^{-3}$ cm^{-1}). The RMS deviation for the other bands are about three orders of magnitude worse. We attribute this to resonances due to the close proximity of modes of the same isotopologue in this region of interest. Further investigations of these resonances are ongoing but out of the scope of this work.

Tables with the fitting results for each band with the comparison to Helminger/ de Lucia can be found in the supplemental material. Also, for each species a list with energy states is provided generated from the lines presented in this work.
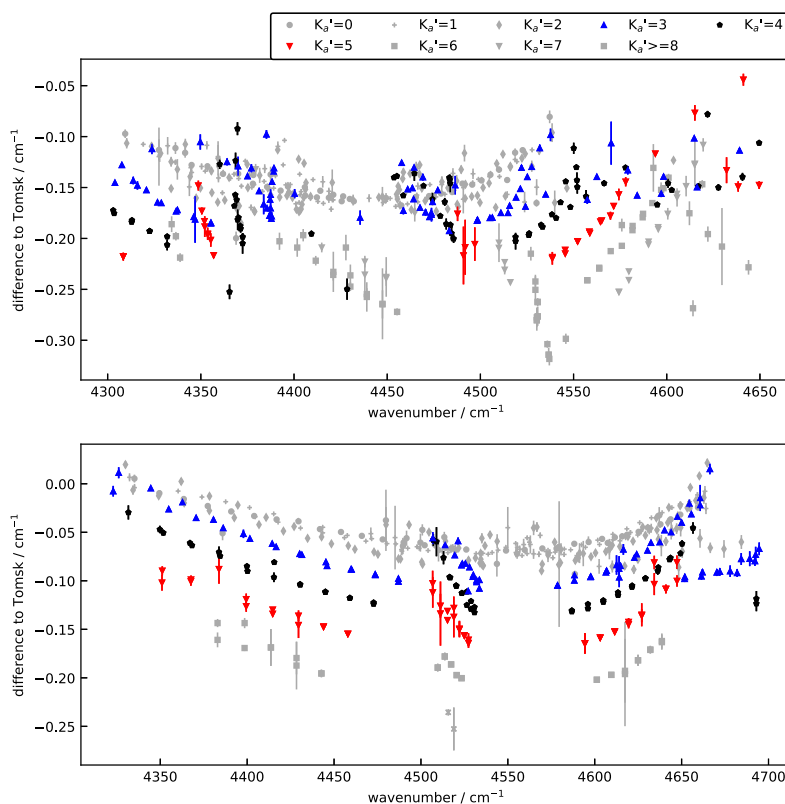
Fig. 3. Difference of the assigned line positions to the theoretical positions from the Tomsk database (Tomsk - observed) exemplary for the $\nu_1 + 2\nu_2$ of DTO and the $2\nu_1$ of HTO. Markers with colours are indicating the lines with quantum numbers $K'_a = 3, 4$ and 5, grey other lines of this band. The vertical lines represent the uncertainty on the line position.
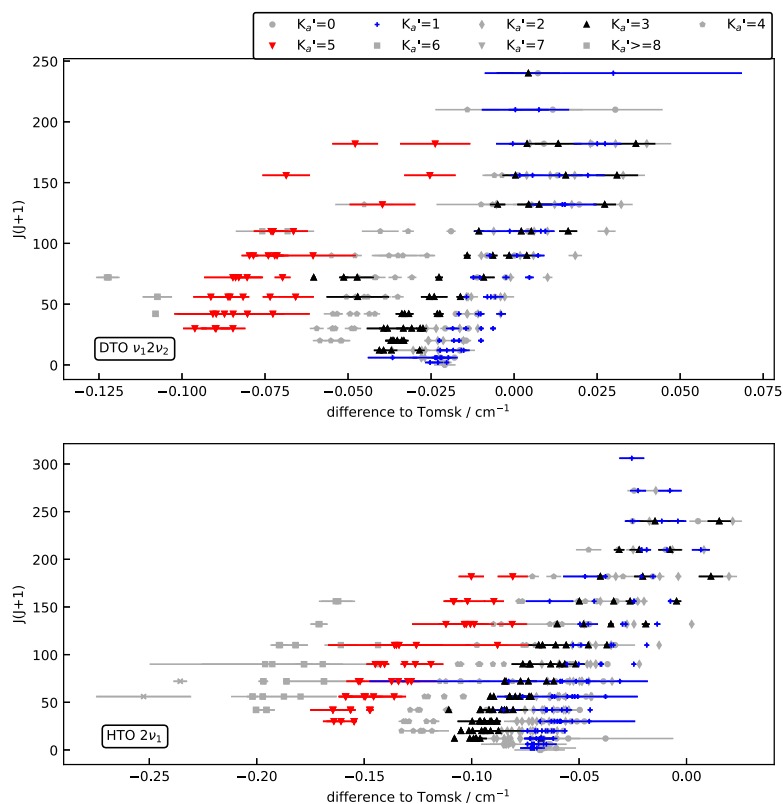

Fig. 4. Difference of the assigned line positions to the theoretical positions from the Tomsk database (Tomsk - observed) exemplary for the $2\nu_1$ of T_2O and HTO. Markers with colours are indicating the lines with quantum numbers $K'_a = 1, 3$ and 5, grey other lines of this band. The *y*-axis is showing the dependence of the differences of the rotational quantum number J'. The horizontal lines represent the uncertainty on the line position.
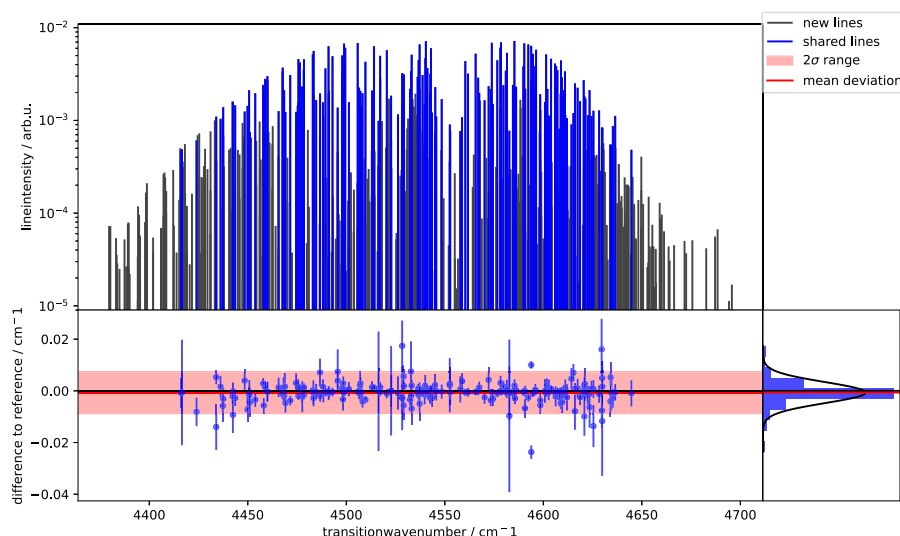
Fig. 5. Line-by-line comparison of the old [21] and new datasets of the $\nu_1+\nu_3$ band of T_2O. For the shared line the differences are plotted in the lower plot and added up to a histogram on the right. A Gaussian fit shows a distribution narrower than a Gaussian for the differences of shared lines. This distribution is result of a mix of a Gaussian distribution for the assignment of blended lines and a smaller Gaussian for isolated lines. The 2σ-range from the Gaussian fit has been highlighted.

3.4. Comparison of the $\nu_1+\nu_3$ band of $T_2^{16}O$ and the $2\nu_1$ band of $HT^{16}O$ to previous assignments

For the comparison of the reassigned $\nu_1+\nu_3$ band of T_2O and the $2\nu_1$ band of HTO to previous assignments, the line lists from earlier works [21,22] of our group have been used. These lines have been analysed from a spectrum obtained from a different sample with 1 GBq activity which corresponds to a 10 times smaller amount. Another feature of the former sample is the large amount of protium which leads to a comparably high signal-to-noise ratio for HTO. The line intensities of the compared data sets shows that the signal-to-noise ratio for this isotopologue is roughly 3 times better when using the 10 GBq sample. For the T_2O species, the improvement is about 55 times larger. Resulting from the enhancement of the SNR, 420 new lines have been assigned to the T_2O band. The HTO band data set has been enlarged by 107 new lines.

To test for consistency of the two measurements, shared lines of both data sets have been compared with regard to their positions. The difference of each line has been statistically analysed in units of cm^{-1} as well as in units of the total uncertainty σ_{total} of the individual line from both data sets. The total uncertainty has been determined by using the individual uncertainty of the line positions from the fitting process of both compared lines and their systematic uncertainty resulting from the calibration of the spectra. The calibration has been performed on different molecules. Therefore, the systematic uncertainty resulting from the positional uncertainty of the HITRAN lines must be included.

$$\sigma_{total} = \sqrt{\left(\sigma_{stat_{old}} + \sigma_{syst_{old}}\right)^2 + \left(\sigma_{stat_{new}} + \sigma_{syst_{new}}\right)^2} \quad (1)$$

The statistical analysis of both bands shows a Gaussian distribution with standard deviations up to 0.80 σ_{total} and minor shifts of up to 6.0×10^{-4} cm^{-1} (both T_2O). In Table 2 a comparison of these values in units of cm^{-1} and σ_{total} is given. In Fig. 5 for the example of the T_2O band, a line-by-line comparison of both datasets is presented. The distribution of the differences (cf. histogram in Fig. 5) is narrower than a Gaussian for the differences of shared lines. This distribution is resulting from a mix of a Gaussian distribution from the assignment of blended lines and a smaller Gaussian from isolated lines.

The higher number of outliers for HTO is probably result of the continuous evolution of the analysis procedure leading to more reliable data for the line positions and their corresponding uncertainties for the most recent data, here the T_2O band.

Table 2

Comparison of the reassigned HTO $2\nu_1$ and T_2O $\nu_1+\nu_3$ bands with previous assignments [21,22]. For the determination of statistical values in units of σ_{total} the individual uncertainty of both compared lines plus their systematic uncertainty have been used. Transitions with differences $> 3 \ \sigma_{total}$ are considered as statistical outliers and have been excluded in the statistics.

Species, band	T_2O, $\nu_1+\nu_3$	HTO, $2\nu_1$
Lines presented	626	454
Lines previous work	206 [21]	361 [22]
New lines	420	107
Shared lines	206	347
Mean difference position (cm^{-1})	-6.1×10^{-4}	5.3×10^{-5}
Std. dev. difference position (cm^{-1})	3.7×10^{-3}	3.4×10^{-3}
Std. dev. difference position (σ_{total})	0.80	0.70
Statistical outliers	2	7

4. Conclusion

After two previously assigned DTO bands from a FTIR spectrum of a sample with an activity of 10 GBq [21], we present the $2\nu_1$, $2\nu_2+\nu_3$ and $\nu_1+\nu_3$ bands of $T_2^{16}O$, the $2\nu_1$ and $\nu_1+2\nu_2$ bands of $DT^{16}O$ and the $2\nu_1$ of $HT^{16}O$ from this spectrum. The presented 2436 lines in the range from 4300 to 4700 cm^{-1} have been assigned with an individual accuracy from 6.8×10^{-2} cm^{-1} up to 3.4×10^{-5} cm^{-1} and a systematic uncertainty of 7.5×10^{-4} cm^{-1} resulting from the calibration process.

The $\nu_1+\nu_3$ band of T_2O and the $2\nu_1$ band of HTO have been measured and assigned in previous works of our group [21,22]. A cross check shows a good consistency of the compared line positions within their stated uncertainties.

A comparison with the predictions of the Tomsk database, obtained from variation ab initio calculations and base of the assignment, shows for all six band a deviation consisting of a band-specific shift and a shift depending on rotational quantum numbers. These deviations have also been observed in previous analyses [21,28].

The newly presented, accurate data of all three tritiated ^{16}O-water isotopologues in close proximity to each other may be foundation for optical monitoring in the fusion fuel cycle and for environmental sensing. Also, the further extension of the high accurate water isotopologues data base by still sparse data of the tritiated species may give opportunity to the theoretical community to investigate the adiabatic and non-adiabatic contributions.

Declaration of competing interest

Data availability

Data will be made available on request.

Acknowledgements

Appendix A. Supplementary data

Supplementary material related to this article can be found online at https://doi.org/10.1016/j.jms.2023.111859.

References

[1] A. Lokhov, S. Mertens, D.S. Parno, M. Schlösser, K. Valerius, Probing the neutrino-mass scale with the KATRIN experiment, Ann. Rev. Nucl. Part. Sci. 72 (2022) 259–282, http://dx.doi.org/10.1146/annurev-nucl-101920-113013.

[2] M. Aker, et al., KATRIN Collaboration Collaboration, Direct neutrino-mass measurement with sub-electronvolt sensitivity, Nat. Phys. 18 (2) (2022) 160–166, http://dx.doi.org/10.1038/s41567-021-01463-1, arXiv:2105.08533.

[3] T. Tanabe (Ed.), Tritium: Fuel of Fusion Reactors, Springer, Tokyo, Japan, 2018.

[4] N.F. Zobov, O.L. Polyansky, C.L. Sueur, J. Tennyson, Vibration-rotation levels of water beyond the Born-Oppenheimer approximation, Chem. Phys. Lett. 260 (3) (1996) 381–387, URL http://www.sciencedirect.com/science/article/pii/000926149600872X.

[5] O.L. Polyansky, R.I. Ovsyannikov, A.A. Kyuberis, L. Lodi, J. Tennyson, N.F. Zobov, Calculation of rotation–vibration energy levels of the water molecule with near-experimental accuracy based on an ab initio potential energy surface, J. Phys. Chem. A 117 (39) (2013) 9633–9643, http://dx.doi.org/10.1021/jp312343z.

[6] K.-F. Lai, V. Hermann, T. Trivikram, M. Diouf, M. Schlösser, W. Ubachs, E. Salumbides, Precision measurement of the fundamental vibrational frequencies of tritium-bearing hydrogen molecules: T_2, DT, HT, Phys. Chem. Chem. Phys. 22 (16) (2020) 8973–8987.

[7] T. Furtenbacher, R. Tóbiás, J. Tennyson, O.L. Polyansky, A.A. Kyuberis, R.I. Ovsyannikov, N.F. Zobov, A.G. Császár, The W2020 database of validated rovibrational experimental transitions and empirical energy levels of water isotopologues. II. $H_2^{17}O$ and $H_2^{18}O$ with an update to $H_2^{16}O$, J. Phys. Chem. Ref. Data 49 (4) (2020) 043103.

[8] J.S. Watson, C.E. Easterly, J.B. Cannon, J.B. Talbot, Environmental effects of fusion power plants. Part II: Tritium effluents, Fusion Technol. 12 (3) (1987) 354–363, http://dx.doi.org/10.13182/FST87-A25068.

[9] M.B. Kalinowski, Uncertainty and range of alternatives in estimating tritium emissions from proposed fusion power reactors and their radiological impact, J. Fusion Energy 12 (1) (1993) 157–161, http://dx.doi.org/10.1007/BF01059372.

[10] M. Velarde, L. Sedano, J. Perlado, Dosimetric impact evaluation of primary coolant chemistry of the internal tritium breeding cycle of a fusion reactor DEMO, Fusion Sci. Technol. 54 (1) (2008) 122–126, cited By 2, URL https://www.scopus.com/inward/record.uri?eid=2-s2.0-49749120624&partnerID=40&md5=781aaefa458c09580b9347ee33592f81.

[11] F.C. De Lucia, P. Helminger, W. Gordy, H.W. Morgan, P.A. Staats, Millimeter- and submillimeter-wavelength spectrum and molecular constants of T_2O, Phys. Rev. A 8 (1973) 2785–2791, URL https://link.aps.org/doi/10.1103/PhysRevA.8.2785.

[12] P. Helminger, F.C. De Lucia, W. Gordy, P.A. Staats, H.W. Morgan, Millimeter- and submillimeter-wavelength spectra and molecular constants of HTO and DTO, Phys. Rev. A 10 (1974) 1072–1081, URL https://link.aps.org/doi/10.1103/PhysRevA.10.1072.

[13] S. Cope, D. Russell, H. Fry, L. Jones, J. Barefield, Analysis of the fundamental asymmetric stretching mode of T_2O, J. Mol. Spectrosc. 120 (2) (1986) 311–316, URL http://www.sciencedirect.com/science/article/pii/002228528690007X.

[14] S. Cope, D. Russell, H. Fry, L. Jones, J. Barefield, Analysis of the ν_1 fundamental mode of HTO, J. Mol. Spectrosc. 127 (2) (1988) 464–471, URL http://www.sciencedirect.com/science/article/pii/0022285288901348.

[15] H. Fry, L. Jones, J. Barefield, Observation and analysis of fundamental bending mode of T_2O, J. Mol. Spectrosc. 103 (1) (1984) 41–55, URL http://www.sciencedirect.com/science/article/pii/0022285284901449.

[16] O. Ulenikov, V. Cherepanov, A. Malikova, On analysis of the ν_2 band of the HTO molecule, J. Mol. Spectrosc. 146 (1) (1991) 97–103, URL http://www.sciencedirect.com/science/article/pii/002228529190373I.

[17] R.A. Carpenter, N.M. Gailar, H.W. Morgan, P.A. Staats, The ν_2 fundamental vibration-rotation band of T_2O, J. Mol. Spectrosc. 44 (2) (1972) 197–205, URL http://www.sciencedirect.com/science/article/pii/0022285272900999.

[18] M. Tine, D. Kobor, I. Sakho, L. Coudert, Determination of the vibro-rotational constants, the dipole moment's function and the intensities of the HTO's ν_1 (ν_3 by usual convention) band, J. Mod. Phys. 3 (12) (2012) 1945, URL http://dx.doi.org/10.4236/jmp.2012.312243.

[19] M.J. Down, J. Tennyson, M. Hara, Y. Hatano, K. Kobayashi, Analysis of a tritium enhanced water spectrum between 7200 and 7245 cm^{-1} using new variational calculations, J. Mol. Spectros. 289 (2013) 35–40.

[20] K. Kobayashi, T. Enokida, D. Iio, Y. Yamada, M. Hara, Y. Hatano, Near-infrared spectroscopy of tritiated water, Fusion Sci. Technol. 60 (3) (2011) 941–943, http://dx.doi.org/10.13182/FST11-A12570.

[21] V. Hermann, M. Gaisdörfer, A. Erygina, P. Lingnau, M. Schlösser, F. Hase, J. Orphal, Analysis of the $\nu_1 + \nu_3$ band of $T_2^{16}O$ and the $\nu_1 + \nu_3$ and $2\nu_2 + \nu_3$ bands of $DT^{16}O$, Mol. Phys. 120 (15–16) (2022) e2097136.

[22] J. Reinking, V. Hermann, J. Müller, M. Schlösser, F. Hase, J. Orphal, The fundamental ν_3 band of DTO and the $2\nu_1$ overtone band of HTO from the analysis of a high-resolution spectrum of tritiated water vapour, J. Mol. Spectros. 370 (2020) 111295, URL https://www.sciencedirect.com/science/article/abs/pii/S0022285220300631.

[23] F. Hase, B.J. Drouin, C.M. Roehl, G.C. Toon, P.O. Wennberg, D. Wunch, T. Blumenstock, F. Desmet, D.G. Feist, P. Heikkinen, M. De Mazière, M. Rettinger, J. Robinson, M. Schneider, V. Sherlock, R. Sussmann, Y. Té, T. Warneke, C. Weinzierl, Calibration of sealed HCl cells used for TCCON instrumental line shape monitoring, Atmos. Meas. Tech. 6 (12) (2013) 3527–3537, http://dx.doi.org/10.5194/amt-6-3527-2013, URL https://amt.copernicus.org/articles/6/3527/2013/.

[24] F. Hase, Improved instrumental line shape monitoring for the ground-based, high-resolution FTIR spectrometers of the network for the detection of atmospheric composition change, Atmos. Meas. Tech. 5 (3) (2012) 603–610, http://dx.doi.org/10.5194/amt-5-603-2012, URL https://amt.copernicus.org/articles/5/603/2012/.

[25] F. Hase, T. Blumenstock, C. Paton-Walsh, Analysis of the instrumental line shape of high-resolution Fourier transform IR spectrometers with gas cell measurements and new retrieval software, Appl. Opt. 38 (15) (1999) 3417–3422, http://dx.doi.org/10.1364/AO.38.003417, URL http://opg.optica.org/ao/abstract.cfm?URI=ao-38-15-3417.

[26] J. Müller, M. Schlösser, F. Hase, N. Ziegler, R. Grössle, D. Hillesheimer, J. Orphal, Custom-built light-pipe cell for high-resolution infrared absorption spectroscopy of tritiated water vapor and other hazardous gases, Opt. Express 27 (12) (2019) 17251–17261, URL http://www.opticsexpress.org/abstract.cfm?URI=oe-27-12-17251.

[27] J. Reinking, M. Schlösser, F. Hase, J. Orphal, First high-resolution spectrum and line-by-line analysis of the $2\nu_2$ band of HTO around 3.8 microns, J. Quant. Spectrosc. Ra. 230 (2019) 61–64, URL http://www.sciencedirect.com/science/article/pii/S0022407319301657.

[28] V. Hermann, M. Kamrad, J. Reinking, M. Schlösser, F. Hase, J. Orphal, Analysis of the $\nu_1 + 2\nu_2$, $\nu_2 + \nu_3$, $\nu_1 + \nu_3$ and the $2\nu_2 + \nu_3$ bands of $HT^{16}O$, J. Quant. Spectrosc. Ra. 276 (2021) 107881, http://dx.doi.org/10.1016/j.jqsrt.2021.107881.

[29] C. Mikhailenko, Y.L. Babikov, V. Golovko, Information-calculating system spectroscopy of atmospheric gases. The structure and main functions, Atmos. Oceanic Opt. 18 (9) (2005) 685–695.

[30] I. Gordon, L. Rothman, R. Hargreaves, R. Hashemi, E. Karlovets, F. Skinner, E. Conway, C. Hill, R. Kochanov, Y. Tan, P. Wcisło, A. Finenko, K. Nelson, P. Bernath, M. Birk, V. Boudon, A. Campargue, K. Chance, A. Coustenis, B. Drouin, J.-M. Flaud, R. Gamache, J. Hodges, D. Jacquemart, E. Mlawer, A. Nikitin, V. Perevalov, M. Rotger, J. Tennyson, G. Toon, H. Tran, V. Tyuterev, E. Adkins, A. Baker, A. Barbe, E. Canè, A. Császár, A. Dudaryonok, O. Egorov, A. Fleisher, H. Fleurbaey, A. Foltynowicz, T. Furtenbacher, J. Harrison, J.-M. Hartmann, V.-M. Horneman, X. Huang, T. Karman, J. Karns, S. Kassi, I. Kleiner, V. Kofman, F. Kwabia-Tchana, N. Lavrentieva, T. Lee, D. Long, A. Lukashevskaya, O. Lyulin, V. Makhnev, W. Matt, S. Massie, M. Melosso, S. Mikhailenko, D. Mondelain, H. Müller, O. Naumenko, A. Perrin, O. Polyansky, E. Raddaoui, P. Raston, Z. Reed, M. Rey, C. Richard, R. Tóbiás, I. Sadiek, D. Schwenke, E. Starikova, K. Sung, F. Tamassia, S. Tashkun, J. Vander Auwera, I. Vasilenko, A. Vigasin, G. Villanueva, B. Vispoel, G. Wagner, A. Yachmenev, S. Yurchenko, The HITRAN2020 molecular

spectroscopic database, J. Quant. Spectrosc. Radiat. Transfer 277 (2022) 107949, http://dx.doi.org/10.1016/j.jqsrt.2021.107949, URL https://www.sciencedirect.com/science/article/pii/S0022407321004416.

[31] F. James, M. Roos, Minuit - A system for function minimization and analysis of the parameter errors and correlations, Comput. Phys. Comm. 10 (6) (1975) 343–367, URL https://www.sciencedirect.com/science/article/pii/0010465575900399.

[32] H. Partridge, D.W. Schwenke, The determination of an accurate isotope dependent potential energy surface for water from extensive ab initio calculations and experimental data, J. Chem. Phys. 106 (11) (1997) 4618–4639, http://dx.doi.org/10.1063/1.473987.